1-2004

Sympathetic vibration due to co-ordinated crowd jumping

Christopher Y. Tuan
University of Nebraska-Lincoln, ctuan@unomaha.edu

3B2v7.51c GML4.3.1 YJSVI : 5923 Prod.Type:COM pp.1–16(col.fig.:NIL) ED:BVTanuja PAGN: VS SCAN:

ARTICLE IN PRESS

Available online at www.sciencedirect.com

SCIENCE DIRECT®

ACADEMIC PRESS

Journal of Sound and Vibration ▮ (▮▮▮▮) ▮▮▮–▮▮▮

JOURNAL OF SOUND AND VIBRATION

www.elsevier.com/locate/jsvi

Letter to the Editor

Sympathetic vibration due to co-ordinated crowd jumping

Christopher Y. Tuan*

Department of Civil Engineering, Peter Kiewit Institute, University of Nebraska at Lincoln, 1110 South 67th Street, Omaha, NE 68182-0178, USA

Received 11 July 2001; accepted 31 March 2003

1. Introduction

In assembly structures or places where crowds may gather such as dance halls, theaters, gymnasia and stadia, the loading is almost entirely caused by human activities. Structural resonance or near resonance and the resulting vibrations causing discomfort of spectators have often been observed during a rock concert [1] or a sporting event [2,3]. Recent research efforts have focused on developing load models [4] to quantify the dynamic loading effects induced by individuals and groups up to 40 people [5]. The lack of coherence of motion from a large crowd, the so-called "group effect", has been quantified based on simulations [5]. The simulation results and the load models thus developed should be verified against actual field data from assembly structures before they are adopted into building codes and standards.

The upper deck of the University of Wisconsin Football Stadium was instrumented with three accelerometers, and sympathetic vibrations induced by co-ordinated rhythmic jumping of spectators have been monitored for several football seasons. In this study, spectral analyses of the field data were conducted to identify the predominant vibrational mode shape of the upper deck and to assess the group effect based on back-calculated load spectral densities.

Analytical computation of the dynamic responses of a structure depends upon the spatial distribution and temporal variation of the loading, and upon the structural properties, including mode shapes, natural frequencies and damping. The computation also requires a reliable model of the structure to serve as a kinematic transfer function to relate the loading to the responses.

Theoretically, the loading process due to spectator activities is random and three-dimensional. The intensity of each load component varies with the location on the structure (as defined by two co-ordinates) as well as with time. In order to simplify the mathematical treatment of the problem, each load component is treated as a random function of time or a time series. It is conceivable that the three load components involved in any spectator movement are somewhat correlated, nevertheless, they are assumed as if they were mutually statistically independent. A frequency

*Tel.: +1-402-554-2462; fax: +1-402-554-3288.
E-mail address: ctuan@mail.unomaha.edu (C.Y. Tuan).

0022-460X/03/$ - see front matter © 2003 Published by Elsevier Science Ltd.
doi:10.1016/S0022-460X(03)00406-1

response function based on a finite-element model of the upper deck was developed for correlating the simulated loading for co-ordinated rhythmic jumping with the vibration data.

2. The University of Wisconsin Camp Randall Stadium

The upper deck of the U.W. Camp Randall Stadium was built of reinforced concrete in 1966 for a seating capacity of 12 000. As shown in Fig. 1, it is an arc in plan with precast seating supported on 23 large frames labelled with letters A to Z except I, O, and Q. The plane of each frame is shown as a radial line. Each frame is h-shaped with the deck support cantilevered from the single column as shown in Fig. 2. Note that frames H through P lack shaded portion of seating. Frames A–X are symmetric about frame *L* with their front edges at a radius of 166 m (545 ft) from the center of the circular arc. Frames Y and Z were built adjacent to frame X at a reduced radius of 58.5 m (192 ft). Three vertically directed, force-balance-type accelerometers were installed at the top of frame C, bottom of frame C, and top of frame X, as shown in Fig. 1. The scale factor of the accelerometers was ± 2.5 V corresponding to ± 1 g (i.e., 9.8 m/s^2 or 32.2 ft/s^2). The analog signals were digitized at 50 samples/s simultaneously by a data-acquisition unit. Each record contained 1024 data points.

2.1. Modelling the upper deck

The upper deck of the U.W. Camp Randall Stadium was modelled as a space frame with plate elements added at locations for the cast-in-place concrete slabs in the concourse area and the

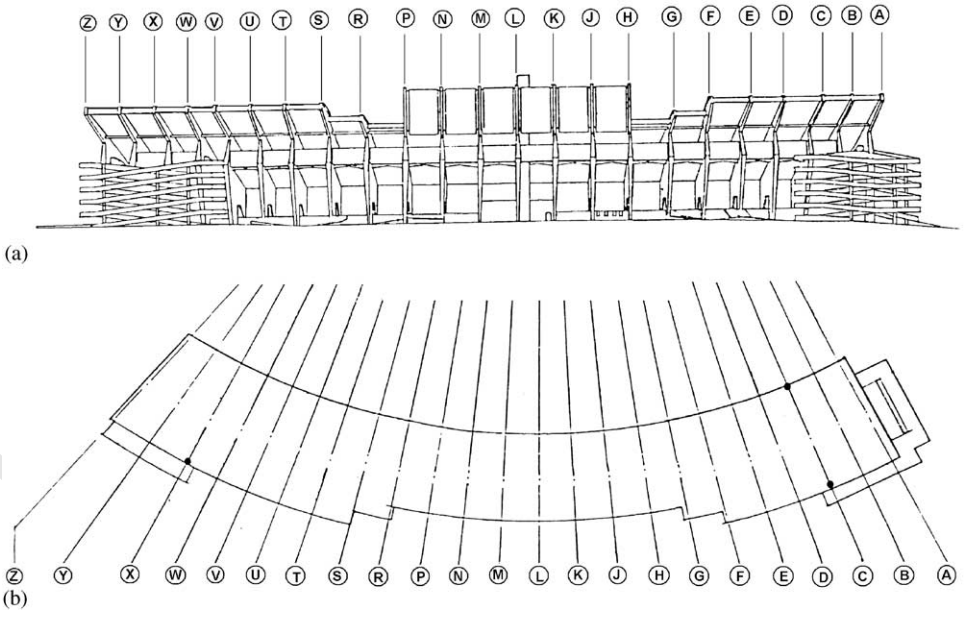

Fig. 1. (a) View toward the back of the University of Wisconsin Stadium and (b) plan view of the upper deck of the U.W. Stadium.

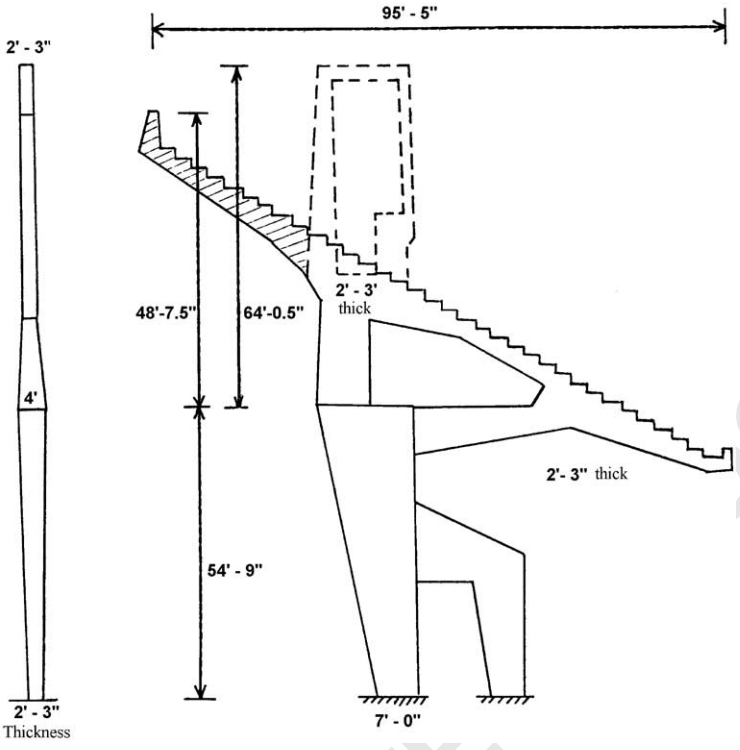

Fig. 2. Typical reinforced concrete frames supporting upper deck of U.W. Stadium.

communication center (i.e., the press box). However, the stiffness of the precast seating units was neglected because each L-shaped seating unit was simply supported at both ends on the main frames and hinged to adjacent units at one-third points along the length by single angles. Each seat-supporting (type 1) frame was idealized with 10 joints and 13 dynamic degrees of freedom (d.o.f.) acting at five lumped masses, while each press-box (type 2) frame with 15 joints and 12 dynamic d.o.f. at five lumped masses. Thus, the dynamic behavior of the upper deck was represented by a total of 292 dynamic d.o.f. The discretization of the type 1 and type 2 frames are given in Fig. 3.

2.1.1. Natural frequencies and mode shapes

The natural frequencies and the associated three-dimensional mode shapes of the first seven modes were obtained by a modal analysis. The periods, natural frequencies and modal masses of these modes are summarized in Table 1. It was noted that the natural frequencies of the various vibrational modes are closely spaced, making identification of the predominant mode difficult.

Typical acceleration-time histories acquired during football games are shown in Fig. 4. Fig. 4a shows a transient vibration under random loading associated with an active event, e.g., a touchdown, while Fig. 4b is a resonant vibration under co-ordinated rhythmic jumping of a crowd. The highest accelerations took place due to resonance when the spectators on the upper deck were jumping in unison to a polka beat played at about 2.2 Hz and lasted for 50 s. Field accelerations of this kind provide valuable response data, which can be used to determine the

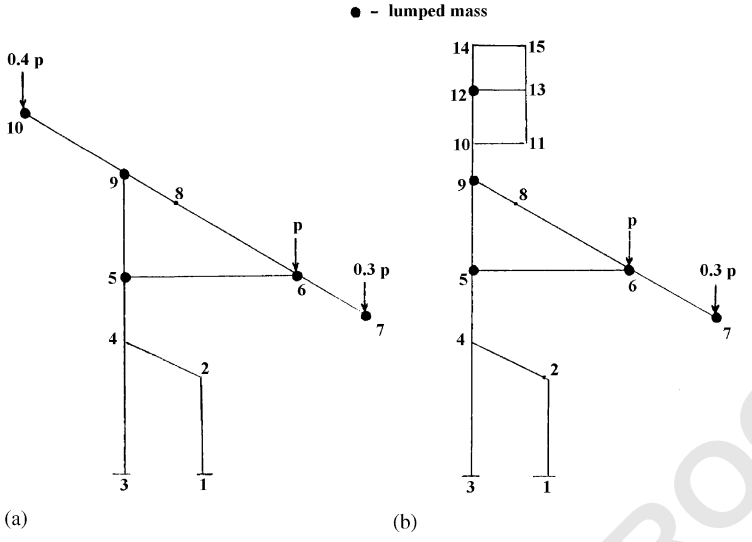

Fig. 3. Finite element models of the supporting frames.

Table 1
Modal analysis results of the first seven modes

Mode	Period, T (s)	Natural frequency, f (Hz)	Modal mass, M^* (kips-s^2/ft)
1	0.50	2.00	103.41
2	0.48	2.10	80.84
3	0.47	2.13	50.44
4	0.46	2.17	71.55
5	0.41	2.41	48.58
6	0.41	2.43	45.24
7	0.36	2.80	21.29

model parameters of the structure as well as to back calculate the loading. The vibration spectra corresponding to the two acceleration-time histories are shown in Figs. 5a and b, respectively. The resonance spectrum reveals that the structural response is almost entirely associated with a single mode of vibration at a natural frequency of around 2.3 Hz. As a result, the upper deck may be assumed to be a single-degree-of-freedom (s.d.o.f.) structural system with little loss of accuracy in computing its resonant behavior.

2.1.2. *Modal damping*

The resonant vibration of the upper deck could be approximated closely with a sinusoidal wave. Typical exponential decay would result when the spectators stopped jumping in unison, as depicted in Fig. 6. Damping ratios estimated from the decaying amplitudes were found to be 2–3% of critical, corresponding to a modal natural frequency of 2.3 Hz.

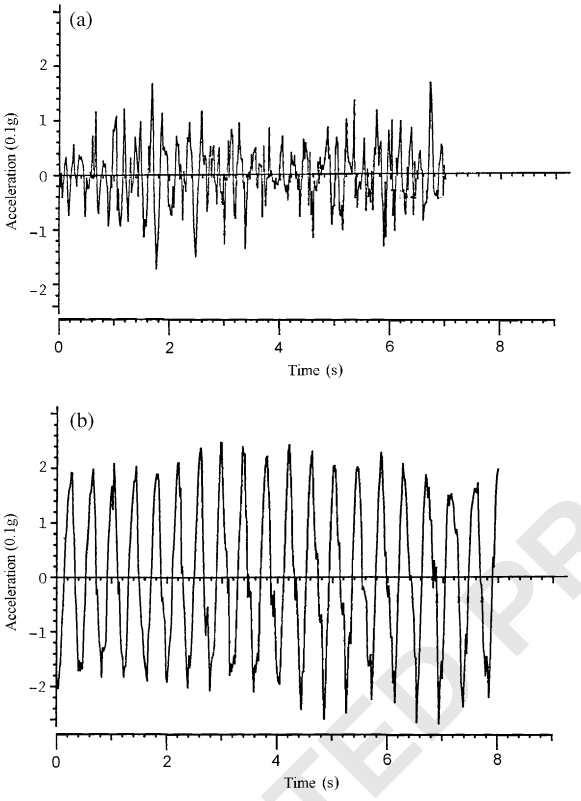

Fig. 4. (a) Acceleration time–history (touchdown response) and (b) acceleration time–history (harmonic vibration).

3. Analysis of the acceleration data

The methods for analysis and presentation of vibration data, in the form of time–histories, were discussed by Bendat and Piersol [6]. The structural vibrations induced by repetitive spectator loading and the loading itself are further assumed herein to be stationary processes, whose statistical properties are invariant with respect to time. The mathematical algorithms based on the theory of random processes are included in Appendix A for quick reference.

3.1. Auto- and cross-correleations

For identification, the acceleration data acquired at the top of frame C are designated with subscript 1, those at the bottom of frame C with 2, and those at the top of frame X with 3. The mean-square values and mean cross-products of the acceleration data during sympathetic vibration of the upper deck are summarized in Table 2. The positive averages of the cross-products indicate that vibrations at the top of frame C and the top of frame X were "in-phase," and the negative values indicate that vibrations at the bottom of frame C were "out-of-phase" with those at the top of frame C and the top of frame X. The acceleration time–history obtained at the three locations (i.e., $i = 1$, 2, and 3) may be expressed as

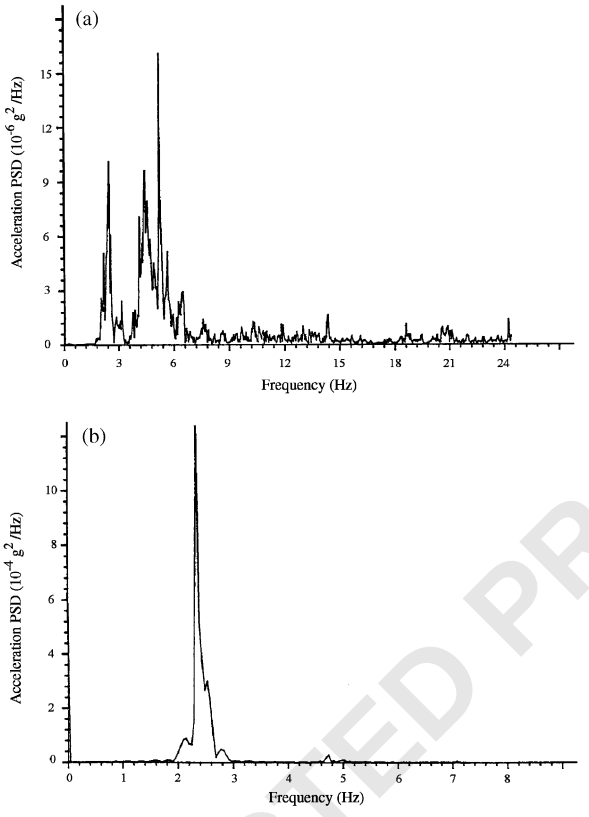

Fig. 5. (a) Response spectrum (touchdown response spectrum) and (b) Response spectrum (resonance spectrum).

$$x_i(t) = A_i \sin(2\pi f t + \theta) \tag{1}$$

and the auto-correlation function of $x_i(t)$ can be expressed as

$$R_i(\tau) = \frac{A_i^2}{2} \cos 2\pi f \tau. \tag{2}$$

Since statistical analyses showed that the acceleration amplitudes A_i followed normal distributions, the expected value or the average of $R_i(0)$ can be computed as

$$E[R_i(0)] = E\left[\frac{A_i^2}{2}\right] = \frac{1}{2}E[A_i^2] = \frac{1}{2}[m_i^2 + \sigma_i^2]. \tag{3}$$

As shown in Table 3, these computed values compare very well with the averages of the mean-square values given in Table 2.

3.2. Power spectral and cross-spectral densities

Power spectral densities S_{11}, S_{22} and S_{33}, and cross-spectral densities S_{12}, S_{23} and S_{13} of the acceleration data obtained during sympathetic vibrations of the 1980–1982 football games are presented in Table 4. The phase shifts and time lags calculated by using Eqs. (A.6) and (A.7) along

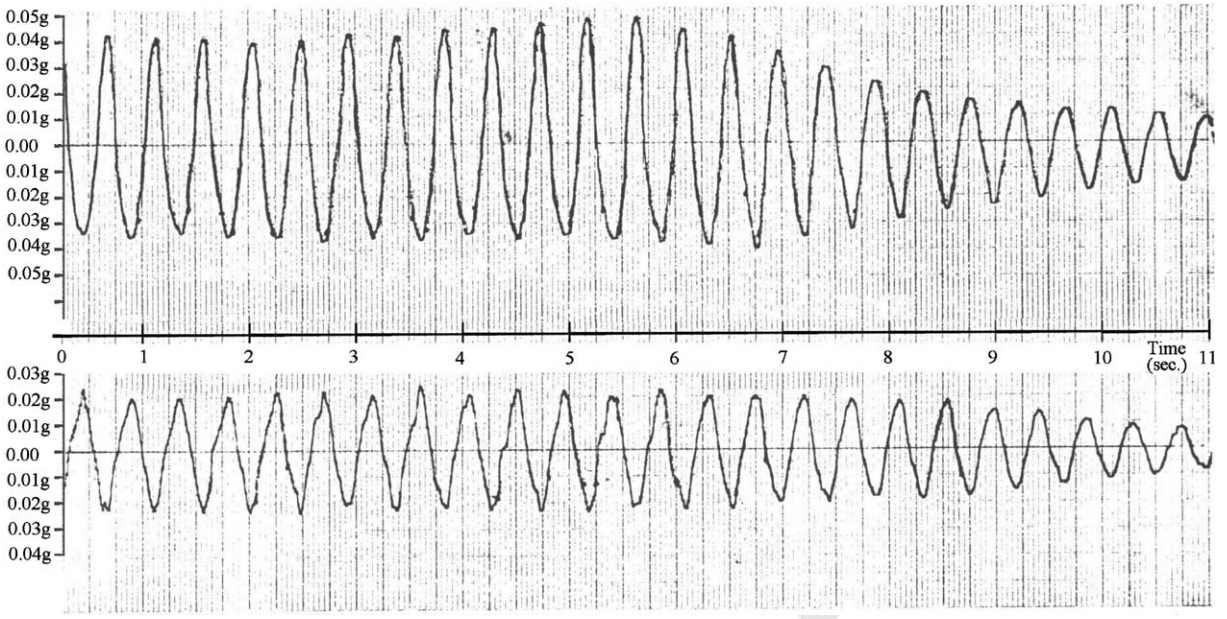

Fig. 6. A typical vibration decay curve ($\xi = 2.3\%$, $f = 2.3$ Hz).

Table 2
Correlations of acceleration data at zero time lag

Football game/season	Mean square ($0.001 \times g^2$)			Mean cross-product ($0.001 \times g^2$)		
	$R_1(0)$	$R_2(0)$	$R_3(0)$	$R_{12}(0)$	$R_{23}(0)$	$R_{13}(0)$
Michigan '80	0.203139	—	0.518475	—	—	0.263197
Michigan '80	0.204680	—	0.796001	—	—	0.358824
Minnesota '80	0.190574	—	1.515470	—	—	0.465961
Minnesota '80	0.287003	—	1.681420	—	—	0.640119
Michigan '81	0.435245	0.831216	2.060340	−0.581295	−1.221430	0.889259
Michigan '81	0.230942	0.431770	0.570196	−0.301776	−0.390938	0.291601
UCLA '81	0.095023	0.191207	0.341723	−0.126444	−0.234811	0.171811
UCLA '81	0.110715	0.213020	0.457277	−0.143940	−0.283998	0.210565
W. Michigan '81	0.434728	0.889593	—	−0.602498	—	—
W. Michigan '81	0.389686	0.838848	—	−0.547237	—	—
Ohio State '81	0.384236	—	0.886720	—	—	0.553280
Ohio State '81	0.371786	—	1.624600	—	—	0.730980
Northwestern '81	0.211151	0.350632	0.551398	−0.238213	−0.350580	0.274611
Northwestern '81	0.266217	0.583495	1.162350	−0.370582	−0.739865	0.490155
Indiana '82	0.174865	0.311363	0.289930	−0.211241	−0.248843	0.183386
Indiana '82	0.133232	0.255280	0.506105	−0.168981	−0.319039	0.237693
Northwestern '82	0.140823	0.215833	—	−0.125095	—	—
Northwestern '82	0.148455	0.271290	—	−0.174238	—	—
Minnesota '82	0.392969	0.682235	0.298864	−0.458940	−0.327663	0.225275
Minnesota '82	0.358091	0.709379	0.821115	−0.483130	−0.733670	0.500283

Table 3
Comparison of average mean-square values

Normal distribution	Top of frame X		Bottom of frame C		Top of frame X	
	m_1	σ_1	m_2	σ_2	m_3	σ_3
	0.021 g	0.007 g	0.028 g	0.011 g	0.036 g	0.013 g
$\frac{1}{2}[m^2+\sigma^2]$	$2.450\times10^{-4}\,g^2$		$4.525\times10^{-4}\,g^2$		$7.325\times10^{-4}\,g^2$	
Avg. of $R(0)$	$2.582\times10^{-4}\,g^2$		$4.839\times10^{-4}\,g^2$		$8.801\times10^{-4}\,g^2$	

Table 4
Acceleration spectral densities at resonant frequency

Football game/season	Power spectral density ($0.01\times g^2$/Hz)			Cross-spectral density ($0.01\times g^2$/Hz)					
	S_{11}	S_{22}	S_{33}	S_{12}		S_{23}		S_{13}	
				C_{12}	Q_{12}	C_{23}	Q_{23}	C_{13}	Q_{13}
Michigan '80	0.5392	—	1.4253	—	—	—	—	0.8741	0.0854
Michigan '80	0.6747	—	2.5170	—	—	—	—	1.3018	0.0004
Minnesota '80	0.6134	—	5.0048	—	—	—	—	1.6726	0.5221
Minnesota '80	1.1235	—	6.5987	—	—	—	—	2.6395	0.6716
Michigan '81	0.5130	1.0054	2.0140	−0.7138	0.0811	−1.4509	−0.0730	1.0268	−0.0640
Michigan '81	0.3674	0.6924	1.0658	−0.5036	0.0271	−0.7983	0.3352	0.5683	−0.2751
UCLA '81	0.2586	0.4852	1.0630	−0.3538	0.0171	−0.7152	−0.0916	0.5241	0.0417
UCLA '81	0.4212	0.7808	1.7594	−0.5726	0.0316	−1.1307	−0.3096	0.8416	0.1814
W. Michigan '81	1.1121	2.1762	—	−1.5534	0.0918	—	—	—	—
W. Michigan '81	0.8869	1.8220	—	−1.2669	0.1007	—	—	—	—
Ohio State '81	0.2014	—	0.1658	—	—	—	—	0.1011	−0.0183
Ohio State '81	0.5586	—	2.6700	—	—	—	—	1.2106	0.1951
Northwestern '81	0.6676	1.0582	1.8402	−0.8368	0.0871	−1.3322	0.5278	1.0066	−0.5165
Northwestern '81	0.4892	1.1358	2.2260	−0.7397	0.0914	−1.5837	−0.0201	1.0314	−0.1176
Indiana '82	0.1459	0.2556	0.3596	−0.1923	0.0182	−0.3061	0.0380	0.2288	−0.0504
Indiana '82	0.0495	0.0829	0.1191	−0.0636	0.0022	−0.1001	−0.0404	0.0788	0.0289
Northwestern '82	0.1604	0.2184	—	−0.1804	0.0405	—	—	—	—
Northwestern '82	0.1566	0.2692	—	−0.2038	0.0165	—	—	—	—
Minnesota '82	0.2515	0.7269	0.2300	−0.6033	0.0640	−0.3318	0.1269	0.2554	−0.1286
Minnesota '82	0.4696	0.9180	1.1053	−0.6553	0.0414	−1.0009	0.1279	0.7094	−0.1366

with the corresponding resonant frequencies are presented in Table 5. The quality of the accelerometer data and the accuracy of spectral analyses can be readily verified by the fact that $\theta_{12}+\theta_{23}=\theta_{13}$ and that $\tau_{12}+\tau_{23}=\tau_{13}$.

3.3. Identification of the mode shape

Let $V_1(t)$, $V_2(t)$ and $V_3(t)$ represent the vertical displacement time–histories at the accelerometer locations on the upper deck and ϕ_1, ϕ_2 and ϕ_3 be the corresponding modal coefficients,

Table 5
Phase shifts and time lags at resonance

Football game/season (s)	Resonant frequency f (Hz)	Phase shift, θ (deg)			Time lag, τ		
		θ_{12}	θ_{23}	θ_{13}	τ_{12}	τ_{23}	τ_{13}
Michigan '80	2.34	—	—	5.58	—	—	0.0132
Michigan '80	2.30	—	—	0.02	—	—	~0
Minnesota '80	2.25	—	—	17.34	—	—	0.0428
Minnesota '80	2.25	—	—	14.28	—	—	0.0353
Michigan '81	2.25	−6.48	2.88	−3.57	−0.016	0.007	−0.009
Michigan '81	2.30	−3.08	−22.78	−25.83	−0.0074	−0.055	−0.0624
UCLA '81	2.30	−2.77	7.30	4.55	−0.0067	0.0176	0.0110
UCLA '81	2.30	−3.16	15.31	12.16	−0.0076	0.0370	0.0294
W. Michigan '81	2.25	−3.38	—	—	−0.0083	—	—
W. Michigan '81	2.25	−4.54	—	—	−0.0112	—	—
Ohio State '81	2.34	—	—	−10.26	—	—	−0.0244
Ohio State '81	2.25	—	—	9.16	—	—	0.0226
Northwestern '81	2.34	−5.94	−21.61	−27.16	−0.0141	−0.0513	−0.0645
Northwestern '81	2.25	−7.04	0.73	−6.50	−0.0174	0.0018	−0.016
Indiana '82	2.34	−5.41	−7.08	−12.42	−0.0128	−0.0168	−0.0295
Indiana '82	2.44	−1.98	21.98	20.14	−0.0045	0.0500	0.0459
Northwestern '82	2.44	−12.65	—	—	−0.0288	—	—
Northwestern '82	2.34	−4.63	—	—	−0.0110	—	—
Minnesota '82	2.34	−6.06	−20.93	−26.73	−0.0144	−0.0497	−0.0635
Minnesota '82	2.30	−3.62	−7.28	−10.90	−0.0087	−0.0176	−0.0263

respectively, in the predominant mode shape of the sympathetic vibration. The vertical displacements may then be expressed in terms of a generalized co-ordinate of the predominant mode, $Y(t)$,

$$V_1(t) = \phi_1^* Y(t), \quad V_2(t) = \phi_2^* Y(t), \quad V_3(t) = \phi_3^* Y(t). \tag{4–6}$$

Differentiating Eqs. (4)–(6) with respect to time twice yields the acceleration time–histories, which would be the same as those acquired by the accelerometers. It follows that the spectral densities of these acceleration time–histories can be expressed as

$$S_{11} = \phi_1^{2*} S_{\ddot{Y}}, \quad S_{22} = \phi_2^{2*} S_{\ddot{Y}}, \quad S_{33} = \phi_3^{2*} S_{\ddot{Y}}, \tag{7-9}$$

where $S_{\ddot{Y}}$ is the power spectral density of the generalized acceleration amplitude evaluated at the resonant frequency. Likewise, the coincident spectral densities of these acceleration time–histories may be expressed as

$$C_{12} = \phi_1^* \phi_2^* S_{\ddot{Y}}, \quad C_{23} = \phi_2^* \phi_3^* S_{\ddot{Y}}, \quad C_{13} = \phi_1^* \phi_3^* S_{\ddot{Y}}. \tag{10-12}$$

Although explicit values of the modal coefficients ϕ_1, ϕ_2 and ϕ_3 are not known, the ratios of these modal coefficients can be computed from the spectral densities given in Table 4:

Table 6
Ratios of mode shape coefficients at resonance

Football game/season	Resonant frequency f (Hz)	ϕ_2/ϕ_1			ϕ_3/ϕ_2			ϕ_3/ϕ_1		
		$-\sqrt{\frac{S_{22}}{S_{11}}}$	$\frac{C_{12}}{S_{11}}$	$\frac{C_{23}}{C_{13}}$	$-\sqrt{\frac{S_{33}}{S_{22}}}$	$\frac{C_{23}}{S_{22}}$	$\frac{C_{13}}{C_{12}}$	$\sqrt{\frac{S_{33}}{S_{11}}}$	$\frac{C_{13}}{S_{11}}$	$\frac{C_{23}}{C_{12}}$
Michigan '80	2.34	—	—	—	—	—	—	1.626	1.621	—
Michigan '80	2.30	—	—	—	—	—	—	1.931	1.929	—
Minnesota '80	2.25	—	—	—	—	—	—	2.856	2.737	—
Minnesota '80	2.25	—	—	—	—	—	—	2.423	2.349	—
Michigan '81	2.25	−1.400	−1.391	−1.413	−1.415	−1.443	−1.438	1.981	2.002	2.033
Michigan '81	2.30	−1.373	−1.371	−1.405	−1.241	−1.153	−1.128	1.703	1.547	1.585
UCLA '81	2.30	−1.370	−1.368	−1.365	−1.480	−1.474	−1.481	2.027	2.027	2.022
UCLA '81	2.30	−1.362	−1.359	−1.344	−1.501	−1.448	−1.470	2.044	1.998	1.975
W. Michigan '81	2.25	−1.399	−1.397	—	—	—	—	—	—	—
W. Michigan '81	2.25	−1.433	−1.428	—	—	—	—	—	—	—
Ohio State '81	2.34	—	—	—	—	—	—	0.907	0.502	—
Ohio State '81	2.25	—	—	—	—	—	—	2.186	2.167	—
Northwestern '81	2.34	−1.259	−1.253	−1.323	−1.319	−1.259	−1.203	1.660	1.508	1.592
Northwestern '81	2.25	−1.524	−1.512	−1.535	−1.400	−1.394	−1.394	2.133	2.108	2.141
Indiana '82	2.34	−1.324	−1.318	−1.338	−1.186	−1.198	−1.190	1.570	1.568	1.592
Indiana '82	2.44	−1.294	−1.285	−1.270	−1.199	−1.207	−1.239	1.551	1.592	1.574
Northwestern '82	2.44	−1.167	−1.125	—	—	—	—	—	—	—
Northwestern '82	2.34	−1.311	−1.301	—	—	—	—	—	—	—
Minnesota '82	2.34	−1.700	−2.399	−1.299	−0.563	−0.456	−0.423	0.956	1.016	0.550
Minnesota '82	2.30	−1.398	−1.395	−1.411	−1.097	−1.090	−1.083	1.534	1.511	1.527

$$\frac{\phi_2}{\phi_1} = \sqrt{\frac{S_{22}}{S_{11}}} = \frac{C_{12}}{S_{11}} = \frac{C_{23}}{C_{13}}, \quad \frac{\phi_3}{\phi_2} = \sqrt{\frac{S_{33}}{S_{22}}} = \frac{C_{23}}{S_{22}} = \frac{C_{13}}{C_{12}},$$
$$\frac{\phi_3}{\phi_1} = \sqrt{\frac{S_{33}}{S_{11}}} = \frac{C_{13}}{S_{11}} = \frac{C_{23}}{C_{12}}. \tag{13-15}$$

These computed ratios are summarized in Table 6. Theoretically, these ratios remained constant between events while the magnitude of $S_{\ddot{Y}}$ varied depending upon the loading intensity. The computed ratios strongly support the "s.d.o.f." approximation and that the resonant vibrations were stationary. The modal coefficient ratios indicate a "rocking" motion of the upper deck was predominant under the rhythmic spectators jumping. The top of frame C and the top of frame X moved in phase, while both moved out-of-phase with the bottom of frame C. The average resonant frequency obtained from Table 6 is 2.31 Hz, along with the average of $\phi_2/\phi_1 = -1.358$, $\phi_3/\phi_2 = -1.301$, and $\phi_3/\phi_1 = 1.890$. These ratios are compared against the ratios of the modal coefficients obtained from the analytic modelling in Table 7.

It is well known that an eigenvalue modal analysis may produce spurious mode shapes and natural frequencies from an analytic model of a massive structure such as a football stadium,

Table 7
Comparison of modal coefficients

Mode	F	ϕ_1	ϕ_2	ϕ_3	ϕ_2/ϕ_1	ϕ_3/ϕ_2	ϕ_3/ϕ_1
1	2.00	0.6795	−0.6806	0.3735	−1.00	−0.55	0.55
2	2.10	−0.6047	0.6173	0.8387	−1.02	1.36	−1.39
3	2.13	0.7890	−0.8079	0.0399	−1.02	−0.05	0.05
4	2.17	−0.4535	0.4695	−0.4086	−1.04	−0.87	0.90
5	2.41	−0.1537	0.1666	1.0000	−1.08	6.00	−6.51
6	2.43	−0.2813	0.3115	−0.6688	−1.11	−2.15	2.38
7	2.80	−0.4041	0.0059	−0.0460	−0.02	−7.80	0.01
Field	2.31	—	—	—	−1.358	−1.301	1.890

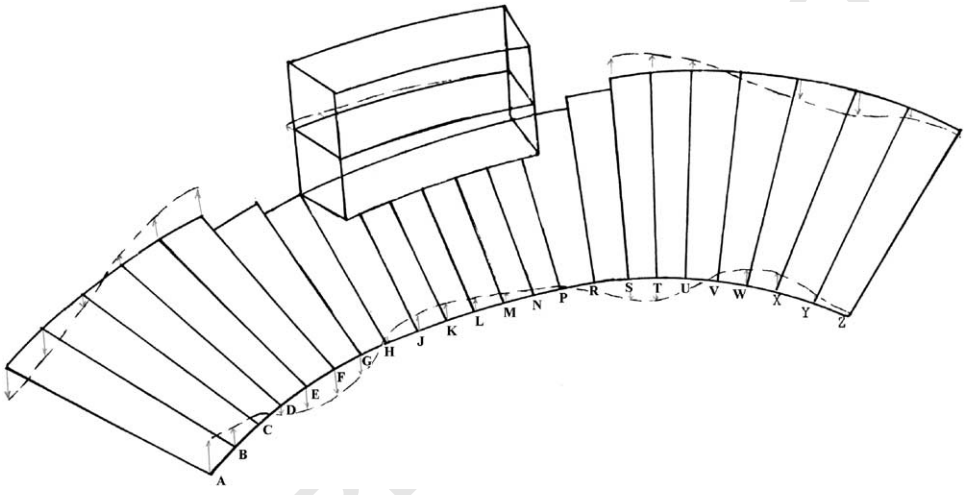

Fig. 7. Qualitative sketch of the sixth modal shape.

especially when there are closely spaced frequencies. In the model used in this study, the mass distribution was approximate due to the "lumping" process while the stiffness distribution of the structure was preserved. Furthermore, the distribution of the loading (i.e., the spectators) may have excited a mode other than the fundamental mode. A careful review of the mode shapes indicates the sixth mode would match the field data most closely with a natural frequency of 2.43 Hz. A qualitative sketch of this mode shape is depicted in Fig. 7. The power spectral density $S_{\ddot{Y}}$ was found to average $7.67 \times 10{-}^2\,\mathrm{g}^2/\mathrm{Hz}$ with the largest magnitude being about $16.5 \times 10{-}^2\,\mathrm{g}^2/\mathrm{Hz}$, if the coefficients of the sixth mode were used.

4. Response of the upper deck by modal analysis

The upper deck of the U.W. Camp Randall Stadium is a multiple-degrees-of-freedom (m.d.o.f.) system, and as such the displacements at any point may be obtained by modal superposition. For

instance, the vertical displacement at point i, $V_i(t)$, can be expressed as

$$V_i(t) = \phi_{i1} Y_1(t) + \phi_{i2} Y_2(t) + \cdots + \phi_{im} Y_m(t), \tag{16}$$

where ϕ_{im} is the modal coefficient in the mth mode shape corresponding to that displacement, if only the first m modes are retained in the analysis. $Y_m(t)$ is the normal co-ordinate or modal amplitude of the mth mode.

The generalized forcing function for the mth mode is the sum of the contributions from the discrete loadings applied at all the applicable dynamic d.o.f.'s:

$$F_m(t) = \sum_j \phi_{jm} P_j(t), \quad j = \text{dynamic d.o.f.}, \tag{17}$$

where $P_j(t)$ may be a horizontal or a vertical force, ϕ_{jm} are the modal coefficients in the mth mode in the directions of the corresponding forces $P_j(t)$. It follows that the power spectral densities of the generalized forcing function of the mth mode can be computed from the power and cross-spectral densities of the discrete loadings $P_l(t)$ and $P_n(t)$, with the participating modal coefficients

$$S_{F_m}(\bar{\omega}) = \sum_l \sum_n \phi_{lm} \phi_{nm} S_{P_l P_n}(\bar{\omega}), \tag{18}$$

where l and n are dummy indices each of which corresponds to a dynamic d.o.f. of the structural system.

4.1. Loading due to rhythmic jumping of a crowd

If the contribution to resonant vibration from the horizontal forces were negligible and the vertical forces were uniformly distributed and coherently applied over the seating deck, the correlation of the loading with the acceleration data can be assessed.

4.1.1. Load models

Tuan [7] proposed a load spectral density model based on a linear regression analysis of load data from rhythmic jumping at about 2 Hz,

$$PSD(\text{lb}^2/\text{Hz}) = 19.6151 \times \psi_x^2\,(\text{lb}^2) - 82570.624, \tag{19}$$

where ψ_x^2 is the mean-square value of the load time–history. The expectation of the mean-square value where n people are jumping in perfect synchronism may be expressed as

$$E\lfloor \psi_x^2 \rfloor = 18\,188 \times n + (180.3)^2 \times C(n, 2). \tag{20}$$

Allen et al. [8] used repeated triangles separated by zero-load intervals to approximate the jumping forces produced by a group of people. Dynamic load factor (defined as peak force amplitude/static weight) of 1.62 was obtained for a "well-co-ordinated" small group of jumpers and 1.31 for a large exercise class, both associated with 1.5–3 Hz forcing frequency. Ebrahimpour and Sack [4,5] measured the periodic jumping forces produced by groups of up to 40 people jumping at 2 and 3 Hz. Based on a loading area of 3.5 ft^2 (0.33 m^2) and average weight of 160 lb (712 N) per person, they recommend using 172 lb (763 N) for one person and 112 lb (498 N) for 10 people for sinusoidal jumping force amplitude per person. These proposed load models with

Table 8
Comparison of load models for rhythmic jumping

Load model	Peak load amplitude (lb)		Mean square (lb^2)		Dynamic load factor		Group effect
	1 person	10 people	1 person	10 people	Small group	Large crowd	
Ref. [10]	197	—	19460	—	1.32	—	0.53[a]
Ref. [1]	—	—	—	—	1.62	1.31	0.81
Ref. [6]	172	112	14720	6272	1.08	0.70	0.65

Notes: Values are given on per person basis; 1 lb = 4.45 N.
[a] Group effect is back calculated from the vibration data.

associated group effects are compared in Table 8, using only the first dominant harmonic of the loading (i.e., for natural frequency of 2.3 Hz).

4.1.2. Estimation of spectator loading based on the field data

The vertical loads acting on the joints 6, 7 and 10 of the mathematical model of the main frames are proportionated according to the tributary seating areas to be P, $0.3P$ and $0.4P$, respectively, as previously shown in Fig. 2. Using Eq. (17), the generalized forcing function $F(t)$ was calculated to be $0.28P$. Using Eqs. (A.8) and (A.11), the power spectral density of $F(t)$ is related to that of the normal co-ordinate $Y(t)$ by

$$S_Y(\bar{\omega}) = \frac{S_F(\bar{\omega})}{K^2\left[1 + (4\xi^2 - 2) \times (\bar{\omega}/\omega) + (\bar{\omega}/\omega)^4\right]}, \tag{21}$$

where $\bar{\omega}$ is a loading frequency, ω the modal frequency, and K the modal stiffness ($K = M\omega^2$). The damping ratio ξ was calculated to be 2% of critical from a vibration decay curve, and the modal mass was calculated to be 45 kips-s^2/ft.

Due to the stationarity of resonant vibration, Eq. (21) can be combined with Eq. (A.12) to yield

$$\frac{S_{\ddot{Y}}(\bar{\omega})}{(\bar{\omega})^4} = \frac{S_F(\bar{\omega})}{M^2\omega^4\left[1 + (4\xi^2 - 2) \times (\bar{\omega}/\omega) + (\bar{\omega}/\omega)^4\right]}. \tag{22}$$

With $S_F(\bar{\omega}) = (0.28)^2 S_P(\bar{\omega})$, the power spectral density of $P(t)$ can be evaluated for the case of resonance (i.e., $\bar{\omega} = \omega$) with $S_{\ddot{Y}} = 16.5 \times 10^{-2}$ g^2/Hz as follows:

$$(32.2)^2 \times (16.5 \times 10^{-2}) = \frac{(0.28)^2 S_P(\bar{\omega})}{(45)^2(1 - 1.9984 + 1)}, \tag{23}$$

where $(32.2)^2$ is required to convert g^2/Hz to ft^2/s^3. As a result, the power spectral density of $P(t)$ is calculated to be 7070 $kips^2$/Hz. This spectral density would correspond to the vertical loading produced by rhythmic jumping of a group of 150 spectators in perfect synchronism.

On the other hand, the loading $P(t)$ acting on joint six of the mathematical model would correspond to a 11.3 m (37 ft) by 8.2 m (27 ft) or 92.9 m^2 (1000 ft^2) of seating area. For a typical stadium, each spectator is provided with a seat 46 cm (18 in) of length and 71 cm (28 in) of tread, or 0.33 m^2 (3.5 ft^2) of seating area. As a ritual, the upper deck was always full of enthusiastic

students jumping to the polka beat played by the marching band to "rock" the stadium, shortly after each football game. Hence, the tributary area would accommodate about 285 spectators. This result indicates that there is a reduction factor of 0.53 associated with the "group effect," which means that perfect synchronism is not likely to be achieved. A review of live loads due to human movements [9] revealed that the 1932 ASA Bulletin [10] recognized this "group effect," stating that a reduction of horizontal forces exists when many people attempt swaying motion together. It was recommended that a factor of 0.75 be applied to account for this effect and that a large crowd could exert no more than 80% of its full strength. However, reduction in dynamic loading due to rhythmic jumping from a large crowd would be quite substantial. The results from the spectral analysis presented herein thus lend support to the load model proposed by Ebrahimpour and Sack [5], with a factor of 0.65 to account for the group effect.

5. Conclusions

The resonant vibrations of the upper deck of the U.W. Camp Randall Stadium induced by coherent jumping of spectators were investigated. Spectral densities of the field accelerations sampled during several football seasons were correlated with a live load spectrum using a three-dimensional finite-element model of the upper deck. Field data were used to identify the predominant mode shape in the structural response and to back calculate the probable load reduction due to the "group effect" in co-ordinated periodic jumping.

The amplitude of the total loading induced from coherent movements of a group of people is likely to be less than the sum of the amplitudes of the constituent loading because of the "group effect." Results from the spectral analysis of the vibration data suggested a reduction factor of 0.53 in loading to be used for periodic jumping from a large crowd. This factor would correspond to the worst-case scenario that the upper deck was fully occupied by the jumpers. The factor would be higher than 0.53 if the deck was only partially full. Therefore, this finding is consistent with the 0.65 factor from the experimental data reported by Ebrahimpour and Sack [5].

Appendix A. Review of random vibrations

A.1. Correlation and spectral density functions

A.1.1. Auto- and cross-correleation functions

The auto-correlation function, $R_x(\tau)$, of a time–history $x(t)$ is the average of the product of the quantity at time t with the quantity at time $t+\tau$ for an observation period T, where τ is a delay in time. If the time–history is stationary, the auto-correlation function is a function of τ only. Mathematically, the auto-correlation function is expressed as

$$R_x(\tau) = \frac{1}{T}\int_0^T x(t)^* x(t+\tau)\,\mathrm{d}t, \quad T \to \infty. \tag{A.1}$$

The cross-correlation of two different stationary time–histories obtained simultaneously, $x(t)$ and $y(t)$, is the average of the product of x at time t and y at time $t+\tau$ for an observation period

T,

$$R_{xy}(\tau) = \frac{1}{T}\int_0^{\mathrm{T}} x(t)^* y(t+\tau)\,\mathrm{d}t, \quad T \to \infty. \tag{A.2}$$

Auto- and cross-correlation functions detect the existence of strong dependence of the one time–history upon the other at specific time lapses τ. It follows that $R_x(0)$ is simply the mean-square value of the time–history $x(t)$. In Eqs. (A.1) and (A.2), the observation period $T = nh$, where $n = 1024$ is the number of data points in $x(t)$, and $h = 0.02$ s is the sampling time interval.

A.1.2. Power spectral and cross-spectral density functions

These functions define the frequency composition of the data. As the auto-correlation and the power spectral density functions are Fourier transform pairs, so are the cross-correlation and cross-spectral density functions. The power spectral density function is computed as

$$S_x(f) = 4\int_0^T R_x(\tau)\exp(-\mathrm{i}2\pi f\tau)\,\mathrm{d}\tau, \quad 0 \leqslant f < \frac{1}{2h}, \tag{A.3}$$

and the cross-spectral density function is computed as

$$S_{xy}(f) = 4\int_0^T R_{xy}(\tau)\exp(-\mathrm{i}2\pi f\tau)\,\mathrm{d}\tau, \quad 0 \leqslant f < \frac{1}{2h}, \tag{A.4}$$

where $\mathrm{i} = \sqrt{-1}$. Eqs. (A.3) and (A.4) are computed using the discrete fast Fourier transform algorithm developed by Cooley and Tukey [11] over a finite range of time lag T. The power spectral density of $x_i(t)$ is a real-valued continuous function of frequency which depicts the distribution of the mean-square value of $x_i(t)$ over a frequency range. The cross-spectral density of two time–histories, $x_i(t)$ and $y_i(t)$ sampled simultaneously, is a complex-valued continuous function of frequency

$$S_{xy}(f) = C_{xy}(f) - \mathrm{i}Q_{xy}(f), \tag{A.5}$$

where the real part, $C_{xy}(f)$, is called the coincident spectral density function or cospectrum, and the imaginary part, $Q_{xy}(f)$, is called the quadrature spectral density function or quad-spectrum. The coincident spectral density function depicts the distribution of the average product $x_i(t)$ and $y_i(t)$ over a frequency range. The quadrature spectral density determines the time lags between $x_i(t)$ and $y_i(t)$ as a function of frequency. Specifically, the phase shift of $x_i(t)$ with respect to $y_i(t)$ is obtained by

$$\theta_{xy}(f) = \tan^{-1}\frac{Q_{xy}(f)}{C_{xy}(f)} \tag{A.6}$$

and the corresponding time lag is computed by

$$\tau = \frac{\theta_{xy}(f)}{2\pi f}. \tag{A.7}$$

The cross-spectral density functions $S_{xy}(f)$ and $S_{yx}(f)$ form a complex conjugate pair.

A.2. Analysis of s.d.o.f. response through the frequency domain

The complex frequency response function of a s.d.o.f. system with mass M, coefficient of viscous damping C and stiffness K is given as

$$H(\mathrm{i}\bar{\omega}) = \frac{1}{K[(1-\beta^2) + 2\mathrm{i}\xi\beta]}, \tag{A.8}$$

where ξ is the damping ratio

$$\xi = \frac{C}{2M\omega}, \tag{A.9}$$

ω is the undamped natural frequency of the s.d.o.f. system

$$\omega = \sqrt{\frac{K}{M}} \tag{A.10}$$

and β is the ratio of the loading frequency $\bar{\omega}$ to the system's natural frequency ω.

The magnitude of a complex frequency response function is the "gain" or the "transfer function" of the system. It can be shown that, for a s.d.o.f. system, the power spectral density of the displacement $S_Y(\bar{\omega})$ is related to that of the loading $S_F(\bar{\omega})$ by

$$S_Y(\bar{\omega}) = |H(\mathrm{i}\bar{\omega})|^2 \times S_F(\bar{\omega}). \tag{A.11}$$

Because of stationarity of the resonant vibration, the power spectral density of acceleration can be obtained by

$$S_{\ddot{Y}}(\bar{\omega}) = \bar{\omega}^4 S_Y(\bar{\omega}). \tag{A.12}$$

References

[1] G. Pernica, Dynamic live loads at a rock concert, Canadian Journal of Civil Engineering 10 (1983) 185–191.
[2] C.Y. Tuan, W.E. Saul, Loads due to spectator movements, Journal of Structural Engineering 111 (2) (1985) 418–434.
[3] L.F. Greimann, F.W. Klaiber, Dynamic forces induced by spectators, American Society of Civil Engineers Journal of the Structural Division 104 (ST2) (1978) 348–351.
[4] A. Ebrahimpour, R.L. Sack, Modeling dynamic occupant loads, Journal of Structural Engineering 115 (6) (1989) 1476–1496.
[5] A. Ebrahimpour, R.L. Sack, Design live loads for coherent crowd harmonic movements, Journal of Structural Engineering 118 (4) (1992) 1121–1136.
[6] J.S. Bendat, A.G. Piersol, Random Data: Analysis and Measurement Procedures, Wiley, New York, 1983.
[7] Y.-B. Tuan, Loads due to human movements on assembly structures, Ph.D. Dissertation, Department of Civil and Environmental Engineering, the University of Wisconsin-Madison, 1983.
[8] J.W. Cooley, J.W. Tukey, An algorithm for the machine computation of complex Fourier series, Mathematics of Computation 19 (1965) 297–301.
[9] W.E. Saul, C.Y. Tuan, Review of live loads due to human movements, Journal of Structural Engineering 112 (5) (1986) 995–1004.
[10] Horizontal forces produced by movements of the occupants of a grandstand, ASA Bulletin 3(4) (1932) 123–126.
[11] D.E. Allen, J.H. Rainer, G. Pernica, Vibration criteria for assembly occupancies, Canadian Journal of Structural Engineering 12 (3) (1985) 617–623.